J Incl Phenom Macrocycl Chem (2009) 64:357–365
DOI 10.1007/s10847-009-9574-1

ORIGINAL ARTICLE

Complexation of *N*-methyl-4-(*p*-methyl benzoyl)-pyridinium methyl cation and its neutral analogue by cucurbit[7]uril and *β*-cyclodextrin: a computational study

Abdel Monem M. Rawashdeh · Musa I. El-Barghouthi · Khaleel I. Assaf · Samer I. Al-Gharabli

Received: 9 December 2008 / Accepted: 16 March 2009 / Published online: 2 April 2009

Abstract In this work, molecular dynamics (MD) simulations have been conducted to study the inclusion complexes between cucurbit[7]uril (CB7) and *β*-cyclodextrin (*β*-CD) with *N*-methyl-4-(*p*-methyl benzoyl)-pyridinium methyl cation, and *N*-methyl-4-(*p*-methyl benzoyl)-pyridine in aqueous solutions to gain detailed information about the dynamics and mechanism of the inclusion complexes. The obtained MD trajectories were used to estimate the binding free energy of the studied complexes using the molecular mechanics/Poisson Boltzmann surface area (MM–PBSA) method. Results indicate preference of CB7 to bind to the cationic guest more than the neutral guest, whereas *β*-CD exhibits more or less the same affinity to complex with either species. Furthermore it was interesting to note that *β*-CD forms more stable complexes with both guests than CB7. Average structure of each complex and the distances between the center of masses of the guest and the host were also discussed.

Keywords Cucurbituril · Cyclodextrin · Inclusion complexes · Molecular dynamics · MM–PBSA

A. M. M. Rawashdeh
Department of Chemistry, Yarmuk University, Irbid, Jordan
e-mail: rawash@yu.edu.jo

M. I. El-Barghouthi (✉) · K. I. Assaf
Department of Chemistry, The Hashemite University, P.O. Box 150459, Zarqa 13115, Jordan
e-mail: musab@hu.edu.jo

S. I. Al-Gharabli
Chemical-Pharmaceutical Engineering Department, German-Jordanian University, Amman, Jordan

Introduction

Cucurbiturils (CBs) are a macrocyclic molecules consisting of glycoluril repeated units. CBs are the product of the acidic condensation reaction between glycoluril unit and formaldehyde. They are barrel-shaped hosts with a hydrophobic cavity and a hydrophilic two oxygen-crowned portals [1–4]. Due to these structural features, CBs form inclusion complexes with a variety of guest molecules [5–14]. One of the important features of CBs is that the electrostatic potential (ESP) at both rims of CB is negative. The inner surface of the cavity shows also negative ESP whereas the outer surface is positive [15]. These features make CB as a suitable host candidate for cationic guest molecules.

In general, the forces involved in the binding of molecular guest by (CBs) are believed to be of van der Waals types, hydrophobic interactions, ion-dipole and hydrogen bond interactions [4, 8].

Rawashdeh et al. studied the guest–host interactions in aqueous solutions between CB7 and a family of guests based on the *N*-methyl-4-(*p*-substituted benzoyl)-pyridinium cation. They found that the studied guest molecules form 1:1 inclusion complexes with CB7 and that the guest molecules included into the hydrophobic cavity from proton NMR studies [3].

Molecular dynamic simulations of guest–host interactions are now being used as tools for understanding the complexation process, particularly the driving forces for complex formation as well as the optimal geometries of the resulting complexes. Up to our knowledge there are no detailed studies in the literature concerning the use of molecular dynamics simulations in studying the inclusion complexes for any member of cucurbiturils family. In this work, molecular dynamics (MD) simulations will be

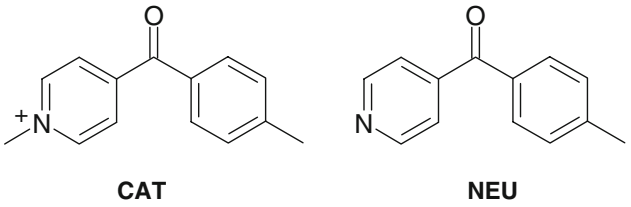

Scheme 1 The studied guest molecules

conducted to study the inclusion complexes between cucurbit[7]uril (CB7) and *N*-methyl-4-(*p*-methyl benzoyl)-pyridinium cation (CAT) and its neutral analogue *N*-methyl-4-(*p*-methyl benzoyl)-pyridine (NEU) (Scheme 1) in aqueous solutions to gain detailed information about the structure and dynamics of the inclusion complexes. Moreover, MM–PBSA will be used to estimate the binding free energy of each guest/CB7 complex. The components of the binding free energies will be also estimated and used to explore the type of guest/host interactions responsible for complex formation, which may provide further insights into the inclusion phenomenon. Also, MD simulations will be carried out for the same set of molecules but included in β-cyclodextrin (β-CD) which has more or less similar cavity volume as CB7 to understand more about the nature of the guest–host interactions between the two macrocyclic compounds. Keeping in mind that although CB7 and β-CD have similar size hydrophobic cavities, the different nature of interaction at the cavity entrance may results in large difference in their guest–host behavior.

Computational methods

The initial molecular geometry of CB7 was obtained using X-ray diffraction data [16]. AM1-BCC charges were used for CB7 [17]. Detailed preparation procedure of β-CD is given in earlier study [18].

The AMBER 8 program was used throughout this work [19] using param 99 [20] (for β-CD) and the general force field parameters sets (for CB7 and the guest molecules) [21]. The electrostatic potential of the guest molecules computed using ab initio HF/6-31G* calculations using the Gaussian 03W package [22]. Atomic charges for guest molecules reproducing these electrostatic potentials were obtained using RESP methodology [23]. All molecules were solvated by a cubic box of TIP3P water molecules [24] with a closeness parameter of 10 Å. Cl^- ions was added when needed to neutralize the system. Periodic boundary conditions were adopted and the particle mesh Ewald method (PME) was used for the treatment of long range electrostatic interaction [25]. The non-bonded cutoff was set to 10.0 Å. Energy minimization was performed for each solvated complex using the conjugate gradient algorithm, heated up to 298 K for 60 ps, followed by 200 ps for achieving equilibration at 298 K and 1 atm. Production runs were carried out for 5 ns; the system was coupled in the NPT ensemble to a Berendsen thermostat at 298 K and a barostat at 1 atm. A 2 fs time step with a saving of the structure every 2 ps was used and the non-bonded pair list was updated every 25 steps. Visualization of the obtained trajectories was done using the VMD program [26]. To obtain average structures, cluster analysis was performed with a high rmsd cutoff (to ensure that all snapshots belong to the same cluster) using the kclust program of the MMTSB package [27], then the structure that corresponds to a conformation closest to the cluster centroid was considered as the average structure.

For MM–PBSA methodology, snapshots were extracted at 2 ps time intervals from the corresponding 5 ns MD trajectories, the explicit water molecules and added ions were removed. Snapshots of the unbound guest molecules, β-CD or CB7 were also taken from the corresponding complex trajectories.

The binding free energy ΔG_{bind} was estimated as given:

$$\Delta G_{\text{bind}} = \Delta E_{\text{gas}} + \Delta G_{\text{solv}} - T\Delta S \quad (1)$$

where ΔE_{gas} is the interaction energy between the guest and host in the gas phase and is given by:

$$\Delta E_{\text{gas}} = \Delta E_{\text{elect}} + \Delta E_{\text{vdW}} \quad (2)$$

while ΔE_{elect} and ΔE_{vdW} represent the guest–host electrostatic and van der Waals interactions, respectively.

The solvation free energy ΔG_{solv} was estimated as the sum of electrostatic solvation free energy ΔG_{PB} and apolar solvation free energy ΔG_{NP}:

$$\Delta G_{\text{solv}} = \Delta G_{\text{PB}} + \Delta G_{\text{NP}} \quad (3)$$

ΔG_{PB} is computed in continuum solvent using PBSA program of AMBER 8, while the ΔG_{NP} was calculated from the solvent-accessible surface area (SASA). A probe radius of 0.14 nm was used to determine the molecular surface. MSMS program was used to calculate the solvent accessible surface area (SASA) required for the estimation of ΔG_{NP} [28] given by:

$$\Delta G_{\text{NP}} = \gamma \text{ SASA} + b \quad (4)$$

where $\gamma = 0.00542$ kcal/(mol Å^2) and $b = 0.92$ kcal/mol.

The change of solute entropy upon complexation, $T\Delta S_{\text{conf}}$, was estimated from normal mode analysis using the NMODE module of the AMBER 8 program.

Since prediction of solute configurational entropy contribution ($T\Delta S_{\text{conf}}$) computed by the normal-mode analysis of the NMODE module in the AMBER 8 is associated with a relatively large error [18, 29], two values of the binding free energies of the complexation process were calculated in this work: ΔG which is the complexation free energy

excluding the solute configurational entropy contribution ($T\Delta S_{conf}$), and ΔG^* which includes the solute configurational entropy contribution ($T\Delta S_{conf}$).

Results and discussion

Two initial orientations of both guest molecules within the β-CD cavity were considered (Fig. 1) in which the pyridinium (or pyridine) ring situated near the narrow rim of β-CD (orientation A) or situated near the wide rim of β-CD (orientation B) while one initial orientation of the guest molecule inside the CB7 was considered since the two rims are equivalent.

Molecular mechanics versus quantum mechanics

In order to examine the applicability of amber parameters used in this study; guest–host binding energy has been calculated using molecular mechanics (MM) and quantum mechanical (QM) calculations. Recent study on β-CD/spironolactone inclusion complex revealed that high level QM method such as B3LYP/6-31G(d,p) should be used to obtain a reliable binding energies [30]. The MM aqueous optimized structures of the complexes were used after removing the solvent molecules. Table 1 shows the binding energies of the studied complexes obtained from MM and B3LYP/6-31G(d,p) methods. Although the obtained values are not close, both methods were able to predict more or less similar affinity for the two host molecules toward the studied guest molecules. Plot of the binding energies obtained from MM versus the values obtained by QM is shown in Fig. 2. The plot is linear with $r^2 = 0.9931$ indicting a high correlation between the two methods. It should be noted here, that only quantum mechanical single point calculations not geometry optimization were carried out. Moreover, the MM optimized geometries obtained in solvent were used to estimate the guest–host binding energies in vacuum. Thus, the values of binding energies obtained in this section will not be discussed to gain information about the inclusion mechanism. Instead, MM–PBSA method was used to estimate binding free energies based on the analysis of the 2,500 snapshots extracted for each system from their MD trajectories. The results are presented later in this article.

Molecular dynamics

The average structures of the corresponding 1:1 complexes obtained from the 5 ns MD trajectories of the complexes are shown in Fig. 3. The average structure of CB7/CAT complexes showed that molecule CAT is included within the hydrophobic cavity with the cationic group interacts with the carbonyl portal in CB7 even if this location of the cationic group leads to a just partial inclusion of the hydrophobic toluene group. The case is changed with the corresponding neutral compound (NEU) where the hydrophobic toluene group is totally inside the cavity leaving the pyridine ring and the guest carbonyl group exposed to the bulk water molecule. The average structure of β-CD/CAT for orientation A involves the penetration of the toluene group into the β-CD cavity, where the pyridinium cation interacts with the surrounding water molecules and the hydroxyl groups at the wide rim of β-CD. The corresponding average structure for orientation B shows that the pyridinium ring is totally immersed in bulk water. Compared to CB7/NEU complex, β-CD/NEU complex shows that the pyridine ring is less exposed to water and included more into the cavity especially in orientation A.

Figure 4 shows plots of the distribution of the distance between the center of mass of the guest and the center of mass of the host. Moreover, the distance as a function of simulation time is superimposed in each plot. Also, the MD-averaged values (and the corresponding standard deviations) for the distance are given in Table 2. Pyridinium or pyridine group moving away from the rim of CB7 to the surrounding water corresponds to the positive axis and moving into the cavity corresponds to the negative axis. For β-CD, guest moving to the wide rim corresponds to the positive axis while moving toward the narrow rim corresponds to the negative axis. It is obvious that in CB7/CAT complex, results show large fluctuation around the average value of distance (standard deviation = 1.8 Å) compared to CB7/NEU complex which shows small

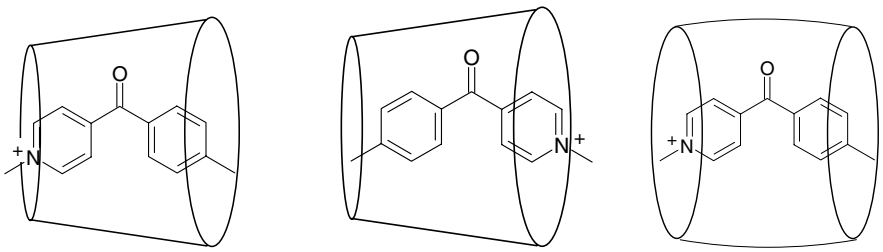

Fig. 1 The initial orientations of the β-CD/guest complexes and CB7 complexes

Table 1 Binding energies (kcal/mol) of the studied complexes obtained from molecular mechanics (MM) and quantum mechanical calculations

Complex	MM	B3LYP/6-31G(d,p)
CB7/CAT	−72.5	−44.5
CB7/NEU	−11.9	2.59
β-CD/CAT[a]	27.6	30.7
β-CD/CAT[b]	−15.1	1.91
β-CD/NEU[a]	−13.3	3.95
β-CD/NEU[b]	−23.6	−3.19

[a] Orientation A

[b] Orientation B

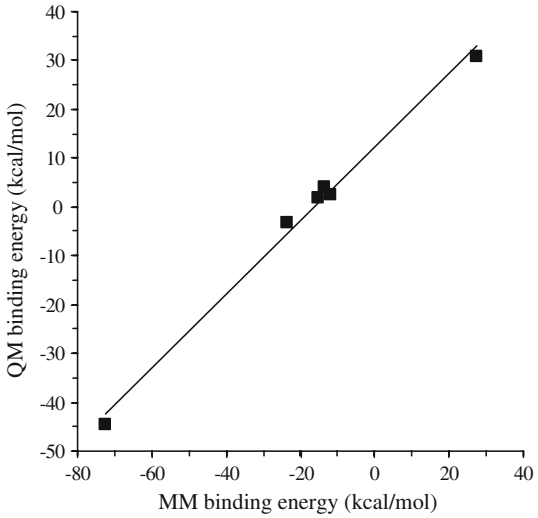

Fig. 2 Plot of the binding energies obtained from QM versus the values obtained by MM

fluctuations (standard deviation = 0.44 Å). Thus most of the sampled complex geometries for CB7/NEU resemble the complex average structure (Fig. 3). This can be explained by the fact that the pyridine and the carbonyl groups in the neutral guest molecule are just hydrogen bond acceptor thus they don't interact via hydrogen bond with CB7 (hydrogen bond acceptor). Thus, it's reasonable that these groups remains in contact with the bulk water to interact via hydrogen bonds letting the hydrophobic toluene reside in the hydrophobic cavity explaining the narrow range of distances sampled. Returning to CB7/CAT complex, the distributions for the distance values (Fig. 4) shows that, as expected, high percent of the sampled distances correspond to the cationic group interacts with CB7 carbonyl portal. Also, it seems that a complex geometry related to distance larger than $\sim+2$ Å, which corresponds to the cationic group interacting with the surrounding water molecule, has a significant probability. Another significant probability but to a lower extent is when the distance is

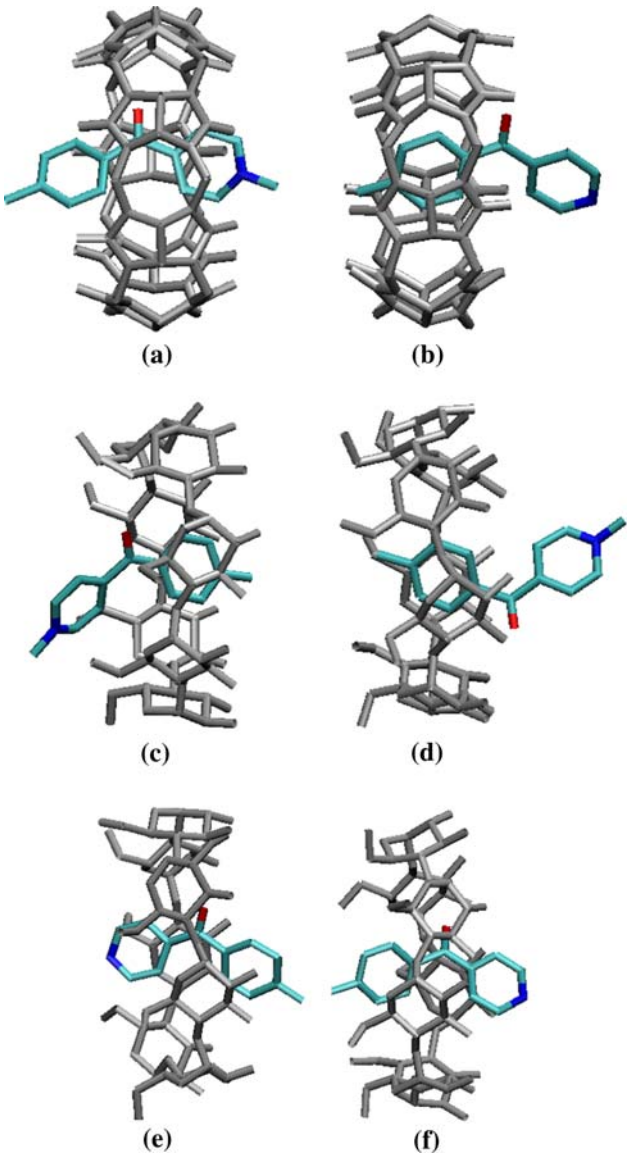

Fig. 3 Average structures of the studied complexes, **a** CB7/CAT, **b** CB7/NEU, **c** β-CD/CAT (orientation A), **d** β-CD/CAT (orientation B), **e** β-CD/NEU (orientation A) and **f** β-CD/NEU (orientation B)

smaller than ~-2 Å, which is related to the inclusion of the cationic group inside the cavity, and the fact that the ESP of the inner surface of the CB cavity is negative [15] can explain the deep inclusion of the cationic group.

In regards to β-CD/CAT complex, Fig. 4 shows that mainly negative distances were sampled for orientation *A* and positive distances for orientation *B*, which correspond in both cases to the cationic group interacting with the surrounding water molecules. However some distances related to the cationic group interacting with β-CD hydroxyl groups rim were observed more for orientation *A* (distance larger than ~-1 Å).

For β-CD/NEU complex, the majority of the sampled complex geometries represent the pyridine group

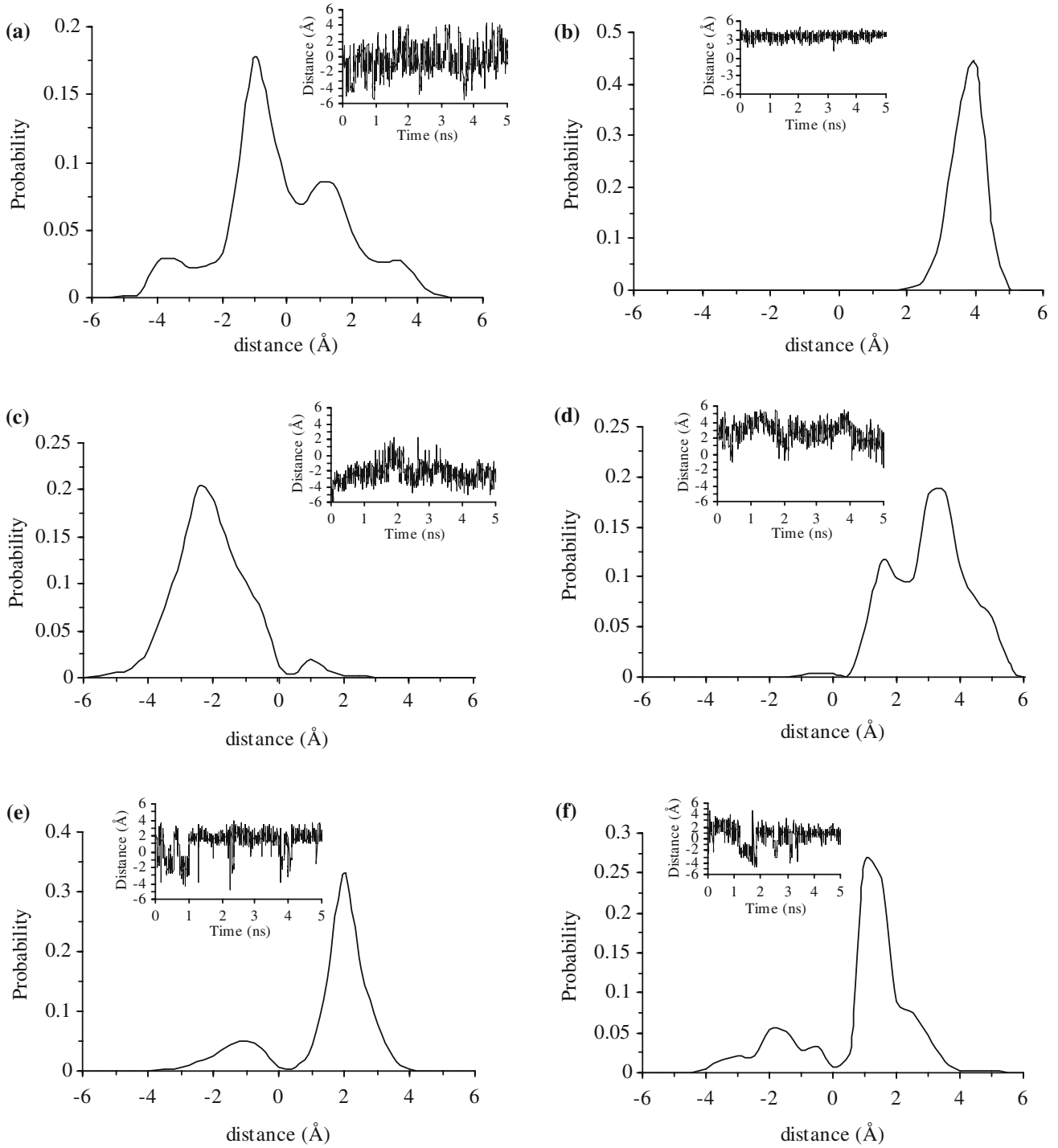

Fig. 4 Distribution functions for the distances between the center of masses of the guest and the host **a** CB7/CAT, **b** CB7/NEU, **c** β-CD/CAT (orientation A), **d** β-CD/CAT (orientation B), **e** β-CD/NEU (orientation A) and **f** β-CD/NEU (orientation B). The distance as a function of simulation time is superimposed in each plot

interacting with the cavity and the hydroxyl groups of β-CD at the narrow rim for orientation *A*. While in orientation *B*, the significant population corresponds to the pyridine group interacting with the bulk water and to a much lower extent to the cavity and the secondary hydroxyl groups of β-CD (distance smaller than ~ -1 Å). This can be explained by the smaller size of the narrow rim of β-CD compared to its wide rim which allows closer contact of the pyridine group with the atoms constituting the narrow rim of β-CD in orientation *A*.

Table 2 MD-averaged values (and corresponding standard deviations) for the distance between host–guest center of masses

Complex	CB7/CAT	CB7/NEU	β-CD/CAT[a]	β-CD/CAT[b]	β-CD/NEU[a]	β-CD/NEU[b]
Distance (Å)	−0.40	3.51	−2.30	2.77	1.20	0.54
Standard deviation (Å)	1.81	0.44	1.14	1.15	1.47	1.6

[a] Orientation A

[b] Orientation B

Figure 5 shows superposition of six snapshots extracted from the MD trajectory for each complex superimposed on a representative host structure. Aside from the translational motion discussed above, it seems that the guest molecules exhibit rotational motion inside the cavity of the host. Aside form CB7/CAT complex, Fig. 5 shows tilting of the plane of the guest molecules with respect to the plane of the host. The favored interaction of the cationic groups in CAT with both CB7 rims may explain the lack of tilting movement of CAT inside CB7.

MM–PBSA results

Table 3 lists the binding free energies (kcal/mol) resulting from the MM–PBSA analysis upon the 5 ns MD trajectories for the studied complexes. Results in Table 3 reveal that CB7 forms more stable complex with the cationic guest molecule (CAT) than the neutral molecule (NEU) [$\Delta\Delta G = -8.73$ kcal/mol and with including the configurational entropy became −8.56 kcal/mol ($\Delta\Delta G^*$)]. This reflects the importance of ion-dipole interactions in CB7 inclusion complexes. Inspection of the binding free energy components reveals that the major contribution is the host–guest electrostatic interactions while it is a minor factor in CB7/NEU complex formation ($\Delta\Delta E_{elec}$ between the two complexes = 65.65 kcal/mol). Above results indicate clearly the tendency of CB7 which bear a negative charged carbonyl portal to interact with cationic guest via electrostatic interaction. Moreover, van der Waals interactions do also contribute to the complex stability for both CB7/CAT complex and it's the dominant stabilizing interactions in the case of CB7/NEU. ΔG_{NP} values are negative for both CB7 complexes indicating that the non polar surface term contributes positively to complex stability, though to a much lower extent compared to the electrostatic and van der Waals interactions. Results also indicates unfavorable electrostatic solvation energy (positive ΔG_{PB}) resulting in an overall positive values of the solvation free energy ($\Delta G_{solv} = \Delta G_{PB} + \Delta G_{NP}$) for both CB7 complexes with much more positive value in the case of CB7/CAT

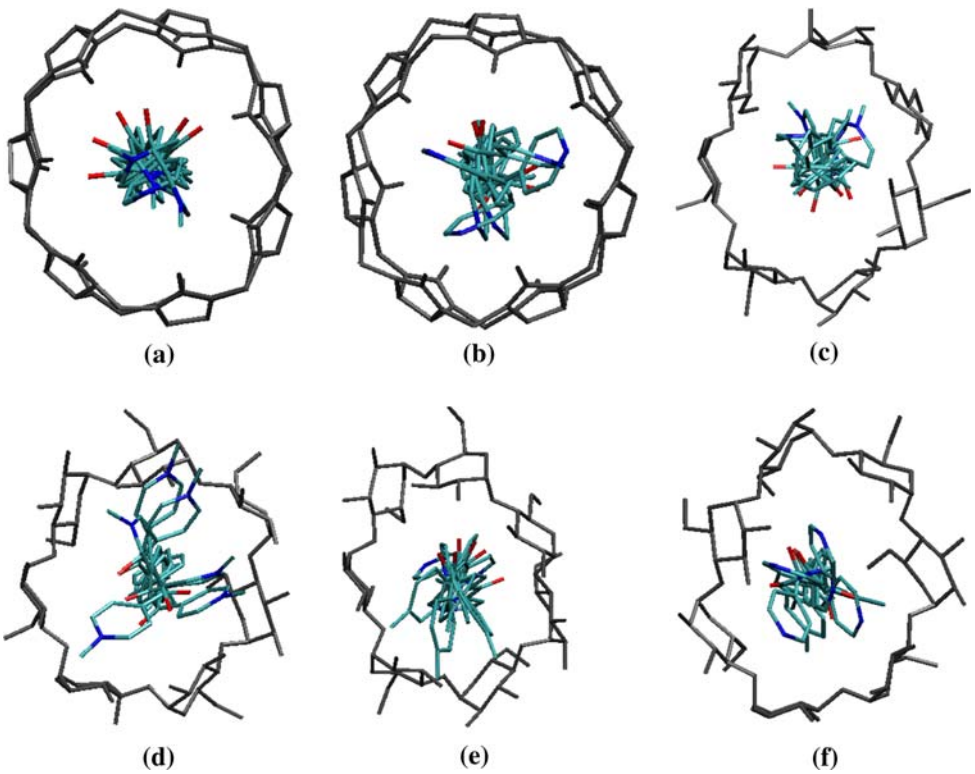

Fig. 5 Dynamics of the 1:1 complexes shown as a clustered molecular display for **a** CB7/CAT, **b** CB7/NEU, **c** β-CD/CAT (orientation A), **d** β-CD/CAT (orientation B), **e** β-CD/NEU (orientation A) and **f** β-CD/NEU (orientation B). Only one conformation of the host molecule is shown for clarity purpose. The drawings include only six structures that refer to the time interval of simulation from 1 to 5,000 ps in 1,000 ps step

Table 3 Binding free energies (kcal/mol) resulting from MM–PBSA analysis of the studied complexes

Energy (kcal/mol)	CB7/CAT	CB7/NEU	β-CD/CAT[a]	β-CD/CAT[b]	β-CD/NEU[a]	β-CD/NEU[b]
ΔE_{elec}	−68.25	−2.6	−13.25	−3.39	−2.74	−4.02
ΔE_{vdW}	−32.89	−26.08	−24.64	−24.78	−25.93	−25.85
ΔG_{NP}	−2.48	−2.15	−2.40	−2.33	−2.33	−2.36
ΔG_{PB}	90.3	26.24	24.37	14.29	14.48	16.86
ΔG_{solv}	87.82	24.09	21.97	11.95	12.15	14.50
ΔG^{c}	−13.32	−4.59	−15.92	−16.21	−16.52	−15.37
$T\Delta S$	−15.24	−15.07	−16.03	−16.18	−15.76	−16.18
ΔG^{*d}	1.92	10.48	0.11	−0.03	−0.76	0.81

[a] Orientation A

[b] Orientation B

[c] $\Delta G = \Delta E_{elec} + \Delta E_{vdW} + \Delta G_{NP} + \Delta G_{PB}$

[d] $\Delta G^{*} = \Delta G^{a} - T\Delta S_{conf}$

complex. This indicates the remarkable reduction of electrostatic interaction of the CAT molecule and the host with the solvent upon complexation leading to unfavorable electrostatic solvation energy (ΔG_{PB}). Examining the average structure in Fig. 3 shows the interaction of the cationic group with the carbonyl groups at CB7 rim and hence less interaction with the surrounding water molecules compared with CB7/NEU complex where the pyridine ring interacts with water molecules explaining the more positive value of ΔG_{PB} in the case of CB7/CAT complex.

For β-CD/CAT complex, results show that orientation B is more favored than orientation A; however the difference between both orientations is so small ($\Delta\Delta G^{*} = 0.14$ kcal/mol) indicating formation of isomeric complexes. Although there is 10 kcal/mol difference in host–guest electrostatic interactions which favored orientation A, but the change is negligible in the estimated binding free energy. This can be explained by looking to the ΔG_{PB} which favors orientation B by around 10 kcal/mol, which is in accordance with the average structures obtained where the pyridinium ring is interacting with the hydroxyl groups of β-CD in orientation A more than B and thus less interaction with the water molecules compared to the free state leading to higher positive value for electrostatic solvation energy.

The differences in binding free energy was found 1.6 kcal/mol between both orientations for β-CD/NEU complex in which orientation B is the most stable.

It is worth noting that unlike CB7 complexes in which the preference of CB7 to bind with the cationic guest molecule is much higher than the neutral guest ($\Delta\Delta G^{*} = -8.56$ kcal/mol), β-CD does not show that remarkable preference (less than 1 kcal/mol favored to the β-CD/CAT complex). This indicates that the selectivity of CB7 toward cationic guest over neutral compared to β-CD. Kim et al. studied the interactions between CB7 with *N*,*N*′-dimethyl-4,4′-bipyridinum (MV^{2+}) using electrochemical method. They showed that CB7 forms more stable inclusion complexes with the charged species [MV^{2+} and the cation radical (MV^{+})] than the fully reduced neutral MV^{0} species. The preference of CB7 to bind with the cationic guest molecule led to design molecular switches. For example, CB6 was found to shuttle along a triamine string by changing the pH value [31]. Also, an electrochemically switchable CB7 based pseudorotaxanes have been synthesized, in which the binding location of CB7 can be controlled via redox conversions [32].

NMODE calculations for both types of complexes, produce negative values of ΔS_{conf} for all studied compounds thus indicating a reduction of guest and host freedom upon complexation. However, NMODE calculations over-estimate the entropy loss upon complexation [18, 27] making the obtained binding free energies (ΔG^{*}) more positive.

Conclusion

Molecular Dynamics simulations and MM–PBSA results indicate the preference of Cucurbit[7]uril to bind to the *N*-methyl-4-(*p*-methyl benzoyl)-pyridinium methyl cation than its neutral analogue, whereas β-CD exhibits more or less the same affinity to complex with either species. Moreover, β-CD forms more stable complexes with both guests than Cucurbit[7]uril. Average structure of each complex indicate that the pyridinium group of the guest molecules interacts with oxygen-crowned portal of Cucurbit[7]uril while pyridine group interacts more with bulk water molecule. The situation is opposite regarding β-Cyclodextrin with the cationic guest molecule in which the pyridinium group interacts mainly with bulk water;

while the neutral pyridine group interacts with bulk water molecules and hydroxyl groups of β-cyclodextrin.

Acknowledgment The authors wish to thank the Hashemite University for the financial support.

References

1. Lagona, J., Mukhopadhyay, P., Chakrabarti, S., Isaac, L.: The cucurbit[*n*]uril family. Angew. Chem. Int. Ed. Engl. **44**, 4844–4870 (2005). doi:10.1002/anie.200460675
2. Pichierri, F.: Density functional study of cucurbituril and its sulfur analogue. Chem. Phys. Lett. **390**, 214–219 (2004). doi:10.1016/j.cplett.2004.04.006
3. Rawashdeh, A.M., Thangavel, A., Sotiriou-Leventis, C., Leventis, N.: Control of the ketone to gem-diol equilibrium by host–guest interactions. Org. Lett. **10**(6), 1131–1134 (2008). doi:10.1021/ol800021r
4. Buschmann, H.J., Mutihacb, L., Mutihaca, R.C., Schollmeyer, E.: Complexation behavior of cucurbit[6]uril with short polypeptides. Thermochim. Acta. **430**, 79–82 (2005). doi:10.1016/j.tca.2005.01.002
5. Mock, W.L., Shih, N.Y.: Structure and selectivity in host–guest complexes of cucurbituril. J. Org. Chem. **51**, 4440–4446 (1986). doi:10.1021/jo00373a018
6. Mock, W.L., Shih, N.Y.: Organic ligand–receptor interactions between cucurbituril and alkylammonium ions. J. Am. Chem. Soc. **110**, 4706–4710 (1988). doi:10.1021/ja00222a031
7. Mock, W.L., Shih, N.Y.: Dynamics of molecular recognition involving cucurbituril. J. Am. Chem. Soc. **111**, 2697–2699 (1989). doi:10.1021/ja00189a053
8. Marquez, C., Hudgins, R.H., Nau, W.M.: Mechanism of host–guest complexation by cucurbituril. J. Am. Chem. Soc. **126**, 5806–5816 (2004). doi:10.1021/ja0319846
9. Kim, H., Jeno, W., Ko, Y.K., Kim, K.: Inclusion of methylviologen in cucurbit[7]uril. Proc. Natl Acad. Sci. USA **99**, 5007–5011 (2002). doi:10.1073/pnas.062656699
10. Moon, K., Kaifer, A.E.: Modes of binding interaction between viologen guests and the cucurbit[7]uril host. Org. Lett. **6**, 185–188 (2004). doi:10.1021/ol035967x
11. Wei, F., Liu, S., Xu, L., Cheng, G., Wu, C., Feng, Y.: The formation of cucurbit[*n*]uril ($n = 6$, 7) complexes with amino compounds in aqueous formic acid studied by capillary electrophoresis. Electrophoresis **26**, 2214–2224 (2005). doi:10.1002/elps.200410260
12. Sindelar, V., Monn, K., Kaifer, A.E.: Binding selectivity of cucurbit[7]uril: bis(pyridinium)-1,4-ylylene versus 4,4′-bipyridinium guest sites. Org. Lett. **6**, 2665–2668 (2004). doi:10.1021/ol049140u
13. Jeon, Y., Kim, S., Ko, Y., Sakamoto, S., Yamaguchi, D., Kim, K.: Novel molecular drug carrier: encapsulation of oxaliplatin in cucurbit[7]uril and its effects on stability and reactivity of the drug. Org. Biomol. Chem. **3**, 2122–2125 (2005). doi:10.1039/b504487a
14. Buschmann, H., Jansen, K., Schollmeyer, E.: The complex formation of α,ω-diols with cucurbituril and α-cyclodextrin the first step to the formation of rotaxanes and polyrotaxenes of the polyester type. Acta Chim. Slov. **46**, 405–411 (1999)
15. Lee, J.W., Samal, S., Selvapalam, N., Kim, H.J., Kim, K.: Cucurbituril homologues and derivatives: new opportunities in supramolecular chemistry. Acc. Chem. Res. **36**, 621–630 (2003). doi:10.1021/ar020254k
16. Kim, J., Jung, I., Kim, S., Lee, E., Kang, J., Sakamoto, S., Yamaguchi, K., Kim, K.: New cucurbituril homologues: syntheses, isolation, characterization, and X-ray structures of cucurbit[*n*]uril ($n = 5$, 7, and 8). J. Am. Chem. Soc. **122**, 540–541 (2000). doi:10.1021/ja993376p
17. Jakalian, A., Bush, B.L., Jack, D.B., Bayly, C.I.: Fast, efficient generation of high-quality atomic charges. AM1-BCC model: I. methods. J. Comput. Chem. **21**, 132–146 (2000). doi:10.1002/(SICI)1096-987X(20000130)21:2<132::AID-JCC5>3.0.CO;2-P
18. El-Barghouthi, M.I., Jaime, C., Al-Sakhen, N.A., Issa, A.A., Abdoh, A.A., Al-Omari, M.M., Badwan, A.A., Zughul, M.B.: Molecular dynamic simulations and MM–PBSA calculations of the cyclodextrin inclusion complexes with 1-alkanols *para*-substituted phenols and substituted imidazoles. J. Mol. Struct. THEOCHEM **853**, 45–52 (2008)
19. Case, D.A., Darden, T.A., Cheatham, T.E., Simmerling, C.L., Wang, J., Duke, R.E., Luo, R.L., Merz, K.M., Wang, B., Pearlman, D.A., Crowley, M., Brozell, S., Tsui, V., Gohlke, H., Mongan, J., Hornak, V., Cui, G., Beroza, P., Schafmerister, C., Caldwell, J.W., Ross, W.S., Kollman, P.A.: AMBER8. University of California, San Francisco (2004)
20. Wang, J., Cieplak, P., Kollman, P.A.: How well does a restrained electrostatic potential (RESP) model perform in calculating conformational energies of organic and biological molecules? J. Comput. Chem. **21**, 1049–1074 (2000). doi:10.1002/1096-987X(200009)21:12<1049::AID-JCC3>3.0.CO;2-F
21. Wang, J., Wolf, R.M., Caldwell, J.W., Kollman, P.A., Case, D.: Development and testing of a general amber force field. J. Comput. Chem. **25**, 1157–1174 (2004). doi:10.1002/jcc.20035
22. Frisch, M., Trucks, G., Schlegel, H., Scuseria, G., Robb, M., Cheeseman, J., Montagomery, J., Verven, J.R., Kudin, K., Burant, J., Iyenger, S., Tomasi, J., Barone, V., Mennucci, B., Cossi, M., Scalmani, G., Rega, N., Petersson, G., Nakatsuji, H., Hada, M., Toyota, K., Fukuda, R., Hasegawa, J., Ishida, M., Nakajima, T., Honda, Y., Kitao, O., Nakai, H., Klene, M., Li, X., Konx, J., Hratchian, H., Cross, J., Adamo, C., Jaramillo, J., Gomperts, R., Stratmann, R., Yazyev, O., Austin, A., Cammi, R., Pomelli, C., Ochterski, J., Ayala, P., Moromuka, K., Voth, G., Salvador, P., Dannenberg, J., Zakrzewski, V., Dapprich, S., Daniels, A., Strain, M., Farkas, O., Malick, D., Rabuck, A., Raghavachari, K., Foresman, J., Ortiz, J., Cui, Q., Baboul, A., Clifford, S., Cioslwski, J., Setvanov, B., Liu, G., Liashenko, A., Piskorz, P., Komaromi, I., Marton, R., Fox, D., Keith, T., Al-Laham, M., Peng, C., Nanayakkara, A., Challacombe, M., Gill, P., Johnson, B., Chen, W., Wong, M., Gonzalez, C., Pople, J.: Gaussian 03 revision A.1. Gaussian, Inc., Pittsburgh (2003)
23. Bayly, C.I., Cieplak, P., Cornell, W.D., Kollman, P.A.: A well behaved electrostatic potential based method using charge restraints for determining atom-centered charges. The RESP model. J. Phys. Chem. **97**, 10269–10280 (1993). doi:10.1021/j100142a004
24. Jorgensen, W., Chanrasekhar, J., Madura, J., Klein, M.: Comparison of simple potential functions for simulating liquid water. J. Chem. Phys. **79**, 926–935 (1983). doi:10.1063/1.445869
25. Darden, T., York, D., Pederson, L.: Particle mesh Ewald-an Nlog(N) methods for Ewald sums in large systems. J. Chem. Phys. **98**, 10089–10092 (1993). doi:10.1063/1.464397
26. Humphrey, W., Dalke, A., Schulten, K.: VMD—visual molecular dynamics. J. Mol. Graph. **14**, 33–38 (1996). doi:10.1016/0263-7855(96)00018-5
27. Feig, M., Karanicolas, J., Brooks, C.L.: MMTSB tool set: enhanced sampling and multiscale modeling methods for applications in structural biology. J. Mol. Graph. Model. **22**, 377–395 (2004). doi:10.1016/j.jmgm.2003.12.005

28. Sanner, M.F., Olson, A.J., Spehner, J.C.: Reduced surface: an efficient way to compute molecular surfaces. Biopolymers **68**, 16–34 (2003). doi:10.1002/bip.10270
29. Hou, T., Guo, S., Xu, X.: Predictions of binding of a diverse set of ligands to gelatinase-a by a combination of molecular dynamics and continuum solvent models. J. Phys. Chem. B **106**, 5527–5535 (2002). doi:10.1021/jp015516z
30. Weinzinger, P., Weiss-Greiler, P., Snor, W., Viernstein, H., Wolschann, P.: Molecular dynamics simulations and quantum chemical calculations on β-cyclodextrin–spironolactone complex. J. Incl. Phenom. Macrocycl. Chem. **57**, 29–33 (2007). doi:10.1007/s10847-006-9165-3
31. Mock, W.L., Pierpont, J.: A cucurbituril-based molecular switch. J. Chem. Soc. Chem. Commun. 1509–1511 (1990). doi:10.1039/c39900001509
32. Sobransingh, D., Kaifer, A.E.: Electrochemically switchable CB7 based pseudorotaxanes. Org. Lett. **8**, 3247–3250 (2006). doi:10.1021/ol061128+